



Characteristics of the horizontal and vertical distributions of dimethyl sulfide throughout the Amundsen Sea Polynya



Intae Kim^a, Doshik Hahm^{b,*}, Keyhong Park^{c,*}, Youngju Lee^c, Jung-Ok Choi^c, Miming Zhang^d, Liqi Chen^d, Hyun-Cheol Kim^e, SangHoon Lee^c

^a Marine Radionuclide Research Center, Korea Institute of Ocean Science and Technology, Ansan 15627, South Korea

^b Department of Oceanography, Pusan National University, Busan 46241, South Korea

^c Division of Polar Ocean Sciences, Korea Polar Research Institute, Incheon 21990, South Korea

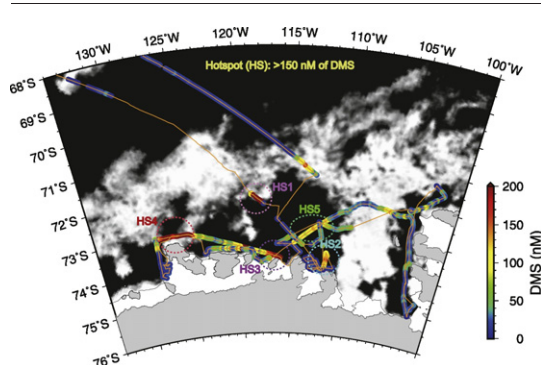
^d Key Laboratory of Global Change and Marine-Atmospheric Chemistry, Third Institute of Oceanography, Xiamen 361005, PR China

^e Unit of Arctic Sea-Ice Prediction, Korea Polar Research Institute, Incheon 21990, South Korea

HIGHLIGHTS

- Recent distributions of DMS were investigated throughout the Amundsen Sea.
- DMS hotspots (>150 nM) in the polynya were observed during the austral summer.
- Trends of DMS and $\Delta O_2/Ar$ were indistinct between the sea ice zone and polynya.

GRAPHICAL ABSTRACT



ARTICLE INFO

Article history:

Received 6 December 2016

Received in revised form 23 January 2017

Accepted 24 January 2017

Available online 29 January 2017

Editor: Jay Gan

Keywords:

Dimethyl sulfide

Membrane inlet mass spectrometer

Amundsen Sea

Southern Ocean

Antarctic polynya

ABSTRACT

We investigated horizontal and vertical distributions of DMS in the upper water column of the Amundsen Sea Polynya and Pine Island Polynya during the austral summer (January–February) of 2016 using a membrane inlet mass spectrometer (MIMS) onboard the Korean icebreaker R/V *Araon*. The surface water concentrations of DMS varied from <1 to 400 nM. The highest DMS (up to 300 nM) were observed in sea ice–polynya transition zones and near the Getz ice shelf, where both the first local ice melting and high plankton productivity were observed. In other regions, high DMS concentration was generally accompanied by higher chlorophyll and $\Delta O_2/Ar$. The large spatial variability of DMS and primary productivity in the surface water of the Amundsen Sea seems to be attributed to melting conditions of sea ice, relative dominance of *Phaeocystis Antarctica* as a DMS producer, and timing differences between bloom and subsequent DMS productions. The depth profiles of DMS and $\Delta O_2/Ar$ were consistent with the horizontal surface data, showing noticeable spatial variability. However, despite the large spatial variability, in contrast to the previous results from 2009, DMS concentrations and $\Delta O_2/Ar$ in the surface water were indistinct between the two major domains: the sea ice zone and polynya region. The discrepancy

* Corresponding authors.

E-mail addresses: hahm@pusan.ac.kr (D. Hahm), keyhongpark@kopri.re.kr (K. Park).

may be associated with inter-annual variations of phytoplankton assemblages superimposed on differences in sea-ice conditions, blooming period, and spatial coverage along the vast surface area of the Amundsen Sea.

© 2017 Elsevier B.V. All rights reserved.

1. Introduction

Dimethyl sulfide (DMS), a volatile trace gas, is mainly derived from biological processes in the surface ocean, such as decomposition of the algal metabolite dimethylsulfoniopropionate (DMSP) (Kettle et al., 1999). The photo-oxidation of DMS in the atmosphere produces Methanesulfonic acid (MSA) and sulfate (SO_4^{2-}) aerosols. These SO_4^{2-} aerosols enhance cloud formation and subsequently Earth's albedo via the backscattering of solar radiation. As a result, the DMS flux at the air-sea boundary directly affects the radiative budget (Charlson et al., 1987); thus, the oceanic DMS cycle can be an important factor in controlling Earth's climate feedback system.

Antarctic polynyas are one of the most productive regions with very high nutrient concentrations as a result of significant terrestrial iron inputs from melting glacier/sea ice or continental shelf sediments, whereas the Southern Ocean mostly suffers from iron limitation (Boyd, 2002). For example, primary productivity in Antarctic polynyas can exceed $2 \text{ g C m}^{-2} \text{ d}^{-1}$, approximately 40% of the total Southern Ocean C-fixation, even though these systems occupy only small coastal areas (Arrigo et al., 1998; Arrigo and Van Dijken, 2003). In addition, Antarctic polynyas can also be a key source region of trace gases, particularly DMS. This can be attributed to an abundance of *Phaeocystis antarctica* (*P. antarctica*) in Antarctic water phytoplankton assemblages, which are known to be an important producer of the DMS precursor, DMSP (Van Boekel and Stefels, 1993; DiTullio and Smith, 1995; DiTullio, 1996). More recently, high concentrations (up to 300 nM) and fluxes of DMS have been documented in the Ross Sea and Amundsen Sea surface that are approximately 2-fold higher in the open polynya waters relative to the mean open ocean (Tortell et al., 2011, 2012). Consequently, large DMS fluxes in the Southern Ocean can play a critical role in climate change. Indeed, several recent modeling studies have predicted that changes in DMS in the Southern Ocean could lead to significant global cooling and, thus, a negative climate feedback loop (Bopp et al., 2004; Cameron-Smith et al., 2011).

Amundsen Sea, west Antarctica, has been known as the most rapidly melting part of the Antarctic ice sheet. This is ascribed to the fact that warm circumpolar deep water (CDW) intrudes the basal layer of the ice-sheet (Jenkins et al., 2010; Jacobs et al., 2011). Thus, a substantial amount of glacial meltwater input in the Amundsen Sea has been known to significantly influence ocean circulation (Randall-Goodwin et al., 2015; Kim et al., 2016), phytoplankton productivity, and biogeochemical cycles (Alderkamp et al., 2012; Gerringa et al., 2012). Previously, Tortell et al. (2012) presented the spatial distributions of DMS in the Amundsen Sea surface in 2009, which accounted for about 1% of the total DMS fluxes of the entire Southern Ocean. However, they only covered the small proportions of the Getz ice shelf (GIS) (the easternmost part of GIS), despite of the huge spatial scale of GIS. For example, it has the third largest ice shelf area ($34,018 \text{ km}^2$) and showing the 2nd largest ice mass loss on the entire Antarctic ice sheet (Rignot et al., 2013). Furthermore, Amundsen Sea has been known to show noticeable short-term (monthly- or seasonal-) temporal variations of hydrographic characteristics and biogeochemistry (Ducklow et al., 2015).

The main research goal of this work is to identify recent regional features of DMS distributions throughout the water column of the Amundsen Sea Polynya region. We measured the horizontal patterns of DMS in the Amundsen Sea surface of 100°W to 130°W , covering the Dotson ice shelf (DIS), Getz ice shelf (GIS), and Pine Island ice shelf (PIIS) (Fig. 1). In addition, to investigate the detailed characteristics of DMS distribution,

we also determined the vertical profiles of DMS in the upper water column of the Amundsen Sea.

2. Materials and method

2.1. Continuous dissolved gas measurements using the membrane inlet mass spectrometer

The research cruise was conducted during the austral summer (Jan. to Feb.) in 2016 onboard the Korean icebreaker R/V *Araon*. DMS concentrations of the Amundsen Sea were measured underway from Jan. 16 to Feb. 11, 2016. The cruise track covered the continental shelf slope region and Dotson trough (DT) crossing the Amundsen polynya. A significant portion of our cruise was also allocated to near-ice shelf surveys (<2 km from ice shelves) adjacent to the DIS, GIS and PIIS (Fig. 1). Surface waters were collected underway from the ship's seawater supply at a nominal depth of 7 m. Membrane inlet mass spectrometry (MIMS) was adopted to measure DMS and O_2/Ar ratios. The MIMS technique directly samples analyte gases from the aqueous phase gases in seawater through a semi-permeable membrane. Because this method does not require headspace equilibration, MIMS enables us to make a near-real time, high frequency continuous observation (e.g., 1 cycle per 30–40 s) of dissolved gases.

In general, the analytical procedures were followed the protocols as described in Tortell (2005). Briefly, the surface water with flow rate $> 300 \text{ mL s}^{-1}$ flowed into a sample reservoir ($\sim 2 \text{ L}$) and the bottom water of the reservoir was pumped by a gear pump to minimize sample alteration due to ambient air, with flow rate of 200 mL min^{-1} . Before passing the circular membrane inlet parts, samples were routed through a coiled heat exchanger (a 6 m-length $1/4''$ stainless steel tube) immersed in cooling water bath, of which temperatures ($2\text{--}4^\circ\text{C}$, varied with respect to the sea surface temperature) were set slightly higher than those of ambient surface waters (Fig. 2). We note that all the sample introduction processes were conducted while maintaining a constant sample temperature by minimizing total line length ($\sim 45 \text{ s}$ for one sample cycle).

The MIMS technique used in this study consists of a quadrupole mass spectrometer with a secondary electron multiplier (SEM) (Hiden 301, UK), vacuumed with diaphragm and turbo pumps, and circular polydimethylsiloxane membrane (with thickness of $20 \mu\text{m}$ and diameter of 3 cm) enclosed in a cuvette (5 cm diameter). The mass spectrometer has an electron impact ionization source. The membrane was replaced once, two weeks after the first measurement. The operating pressure was $< 2 \times 10^{-5}$ Torr. DMS ($m/z = 62$) and other major gases were measured by the SEM detector and Faraday cup, respectively. The settings for the filament current of the ion source and multiplier acceleration voltage were set to $500 \mu\text{A}$ and 1500 V , respectively.

2.2. Discrete sample measurements

The discrete vertical samples were collected in borosilicate glass bottles with ground glass stoppers at 16 CTD stations. To minimize degassing, the bottles were filled with seawater with no headspace and kept in the refrigerator (4°C) until analysis. All samples were measured within 1 h after sampling. Discrete samples were introduced to the system by moving the inlet plastic tubing, which was used to introduce the surface water, from the surface water reservoir to a sample bottle. After flushing the plumbing for 2 min, the outlet plastic tubing was moved to the sample bottle from the sink to recirculate sample waters. All the bottle samples were measured for at least 7 min (> 10 runs).

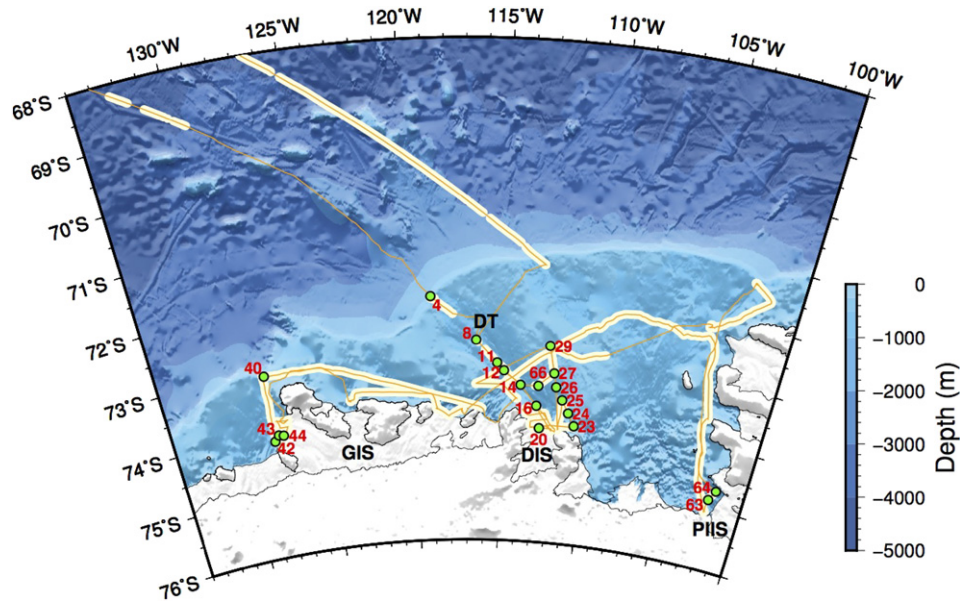


Fig. 1. Map showing cruise track of underway measurements of DMS, $\Delta O_2/Ar$, and fluorescence. Seawater samples for vertical profiles of DMS and O_2/Ar were collected at 20 stations (green filled circle). The station numbers of each CTD cast for bottle sampling are also denoted.

There was no noticeable decrease of measured signals during the recirculation, suggesting no significant change of the sample properties during the measurements.

2.3. Calibration

DMS was calibrated using externally prepared standard solutions. The standard solutions were diluted from pure DMS solution (>99.0%, Sigma-Aldrich) to accommodate the local DMS concentrations. The concentration of standard solutions varied between 1 nM and 100 nM. Methanol (HPLC grade) and filtered DMS-free deep waters (>500 m depth) were used as media solutions for primary- and working-standards, respectively (Stefels, 2009). All the primary stock solutions were sealed by gas-tight clamping with minimum headspace and stored in the refrigerator (4 °C) until analyses were conducted. Then, the primary stocks were diluted to ~520 mL in a glass bottle as working standards right before each measurement. The correlation coefficients (R^2)

of most external calibration curves were >0.92. These DMS calibrations were conducted 1 to 2 times every 24 h.

The O_2/Ar ratios were also calibrated using a deep seawater standard right after each DMS calibration. The equilibrated O_2/Ar standards (single standard) were prepared by gently bubbling fresh air into deep seawater with an aquarium pump for >3 h. During the bubbling, the deep water bottle was kept in the water bath at a constant temperature together with the coiled heat exchanger. A continuous measurement of O_2/Ar during the bubbling suggests that O_2/Ar reaches equilibrium within 40 min.

2.4. Calculating biological oxygen supersaturation, $\Delta O_2/Ar$

Dissolved oxygen (DO) concentrations alone cannot represent the biological production-derived O_2 accurately because DO can be affected by various physical processes as well (e.g., dissolution of air, bubble injection, and changes in water temperature and air pressure). Instead,

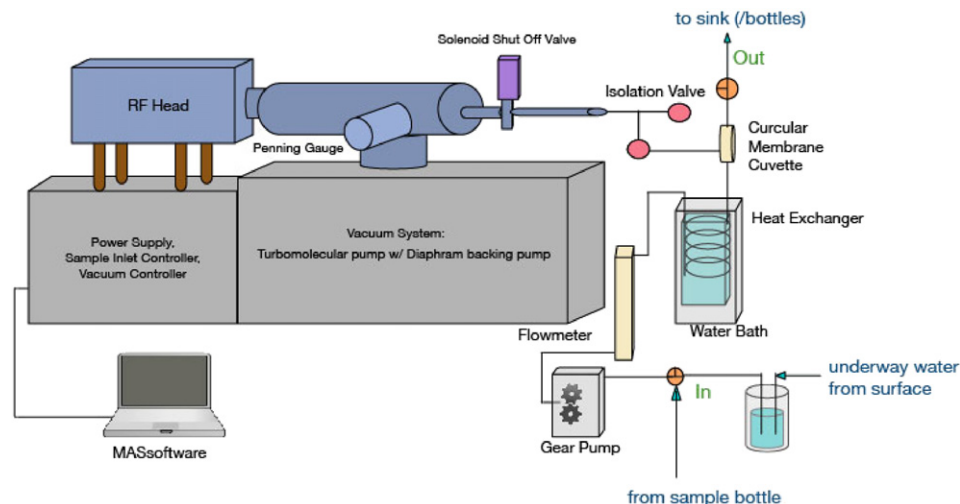


Fig. 2. Schematic of our MIMS-underway measurement system.

because biologically inert Ar has similar solubility and diffusivity to O₂, the amount of only biologically derived O₂ can be quantified by the O₂/Ar ratio (Craig and Hayward, 1987). Biological oxygen supersaturation is defined as follows:

$$\Delta O_2/Ar(\%) = \left\{ (O_2/Ar)_{\text{measured}} / (O_2/Ar)_{\text{saturated}} - 1 \right\} \times 100 \quad (1)$$

where (O₂/Ar)_{measured} and (O₂/Ar)_{saturated} are the ratios of O₂/Ar in the sampled and air-saturated water, respectively.

2.5. Calculating sea-air flux of DMS

We used our surface concentration measurements and shipboard wind-speed data at a height of 10 m to calculate the sea-air flux of DMS. Because atmospheric concentrations are often assumed to be

negligible, we calculated the sea-air exchange of DMS as

$$F_{\text{DMS}} = (1-A) \times k_{\text{DMS}} \times \text{DMS}_{\text{SW}} \quad (2)$$

where A is the fraction of sea surface covered by ice and DMS_{SW} is the concentration of DMS in the surface ocean. k_{DMS} is the piston (gas transfer) velocity calculated as a function of instantaneous wind speed and the temperature dependent Schmidt number (Sc) (Wanninkhof, 1992) and normalized to the Sc for DMS according to Saltzman et al. (1993). We used shipboard daily mean wind speeds.

2.6. Other hydrographic data

Measurements of sea surface chlorophyll *a* fluorescence (used as a proxy for bulk phytoplankton biomass) was continuously recorded

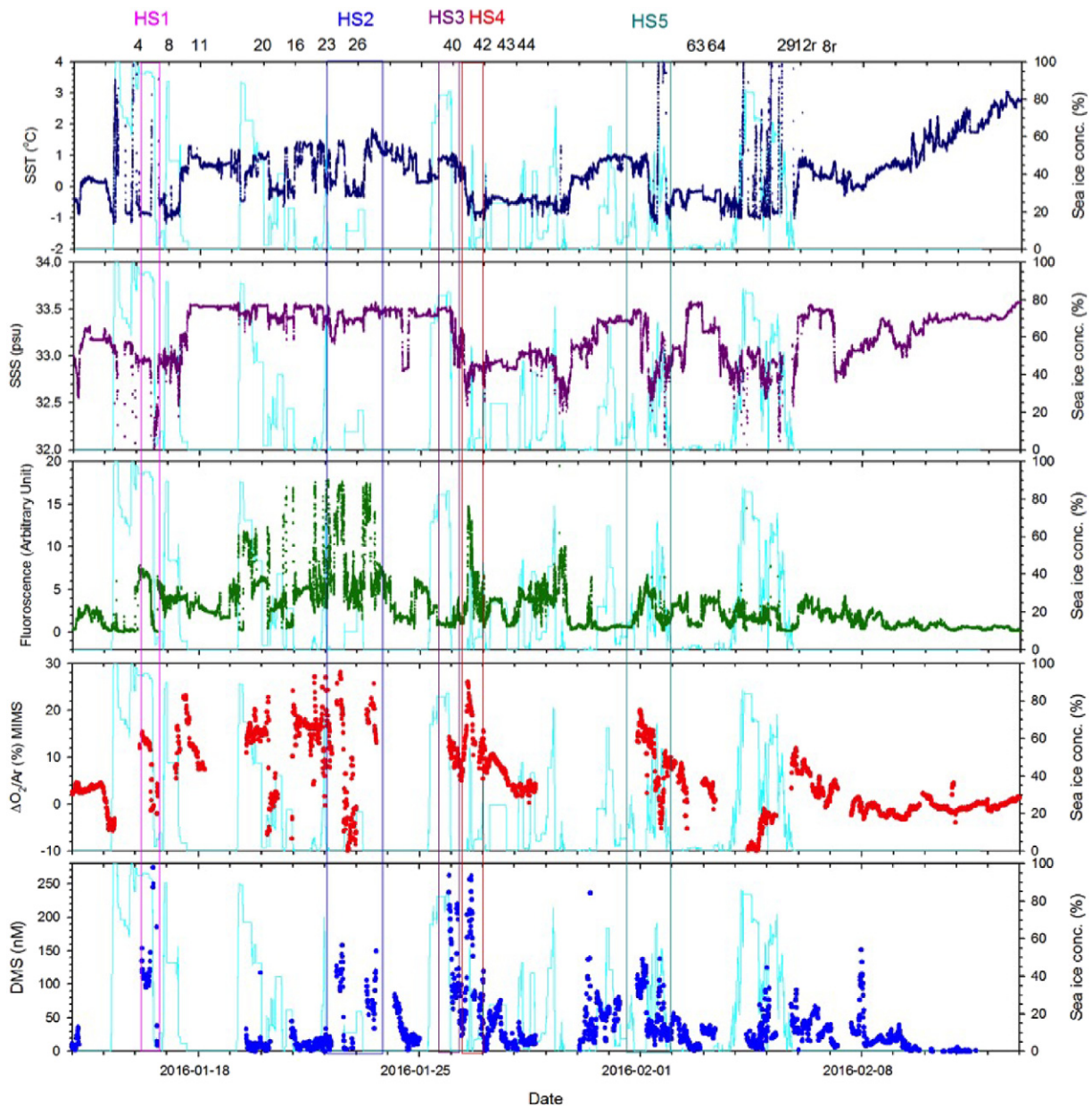


Fig. 3. Time series of SST (navy dots), SSS (purple dots), fluorescence (green dots), $\Delta O_2/Ar$ (%) (red dots), and DMS (blue dots) measured by and MIMS during the entire sampling period with sea-ice concentrations (%). Station numbers are denoted in the top row with the corresponding date.

using the underway fluorometer (Turner 10-AU). Sea ice concentrations along the ship track were obtained from AMSR2 daily sea ice maps (Spreen et al., 2008).

3. Results

3.1. Spatial distributions of DMS and sea-to-air DMS flux in the Amundsen Sea Polynya

Fig. 3 shows the time series of DMS concentrations accompanied by the sea surface temperature (SST), sea surface salinity (SSS), fluorescence (chlorophyll *a*), biological oxygen saturation anomaly ($\Delta O_2/Ar$), and sea ice concentrations. The concentrations of DMS varied greatly from 3 to 400 nM (mean concentration: 37 ± 76 nM) with a median value of 20 nM. $\Delta O_2/Ar$ and fluorescence ranged from -20 – 30% and 0 – 18 (arbitrary unit), respectively, with averages of $4.3 \pm 5.9\%$ and 2.5 ± 2.7 ($\pm 1\sigma$). The highest values of mean DMS were observed on Jan 27–28 in continental shelf regions near the westernmost part of GIS (near station 40), but those of $\Delta O_2/Ar$ and fluorescence were observed on Jan 22–23 along the eastern transect of DT (stations 23 to 25). The DMS concentrations and $\Delta O_2/Ar$ were lower in the PIIS region than those in DIS and GIS regions.

Figs. 4–6 show the spatial distributions of DMS, chlorophyll *a* and $\Delta O_2/Ar$, SST and SSS with sea ice concentrations along the cruise track in the Amundsen Sea surface. As shown in Figs. 3 and 4, several DMS hotspots (referred to as “HS”) were found where DMS concentrations exceed 150 nM. The first DMS hotspot, site HS1, was observed on Jan 16 near the shelf break region in the polynya, while other biological parameters, such as chlorophyll and O_2 production, were not higher than other periods or regions (Figs. 4 and 5).

The HS2 site was observed in the eastern transect of DT and DIS (stations 23 to 25 in Fig. 1). In this region, the highest biomass (fluorescence from 10 to 20, arbitrary unit) (Figs. 3 and 5) was also observed with a sudden increase of DMS (up to 150 nM) relative to the nearby DIS region.

The HS3 site was observed at the eastern part of GIS (Jan 26 to 27, Fig. 3) and the HS4 site was observed near the westernmost part of GIS (around station 40 on Jan 27 to 28, Fig. 3), where the highest values of mean DMS were up to 250 nM. On the way to the eastern part of

Amundsen Sea or PIIS, we also observed noticeably high DMS concentrations in the central polynya region, HS5 (Fig. 4).

However, in other DT or polynya center regions (stations 8 to 16, on Jan 18 to 25; Figs. 1 and 3), DMS concentrations were lower than average DMS concentrations, despite the fact that the cruise track was along the sea ice-free polynya.

The mean DMS flux along our cruise track was 0.085 ± 0.119 mmol $m^{-2} d^{-1}$, with a median value of 0.025 mmol $m^{-2} d^{-1}$. Sea–air gas fluxes varied substantially because of underlying variability in both wind speeds and gas concentrations in the ocean surface. Generally, variability in surface water DMS concentrations was known to be the most important factor for DMS flux variability. However, in our study region, the local wind speed could also be a significant source of DMS flux variation, which had highly varied from 1 to 27 $m s^{-1}$.

3.2. Vertical distributions of DMS in the Amundsen Sea Polynya

Figs. 6 and S1 show the vertical distributions of DMS and $\Delta O_2/Ar$ in the upper water column of the Amundsen Sea. Most DMS concentrations were highest in the surface waters and decreased with depth. The highest DMS concentrations were observed in the surface water of station 4 (vicinity of HS1 site, shelf break region in DT) and stations 24 to 26 (vicinity of HS 4 site, eastern transect of along DT), which was generally consistent with the surface underway results (Figs. 6 and S1).

In the DT region (stations 4, 8, 11, 16, and 20), the DMS concentration was highest at station 4, the sea ice–polynya transition zone near HS1 site, whereas the DMS was closed to 0 nM at station 8 albeit the proximity between station 4 and station 8 (Fig. 6). The sea-ice concentrations (SIC) were $\sim 0\%$ at station 4 but $\sim 50\%$ at station 8 (Fig. 3).

On the eastern side of DT (stations 23 to 26), near HS2 site, the chlorophyll concentrations were highest (Fig. S2). The DMS and $\Delta O_2/Ar$ ratio at the surface ranged from 150 to 200 nM and 10–20%, respectively, and decreased with depth (Figs. 6 and S1).

At station 40, the shelf regions of western GIS in the vicinity of HS4 site, DMS concentrations exceed ~ 100 nM (0–50 m depths) even though fluorescence was comparable to average values. However, when closing to the ice shelf regions, the westernmost part of GIS (stations 42 to 44), the DMS concentrations at the surface were lower than

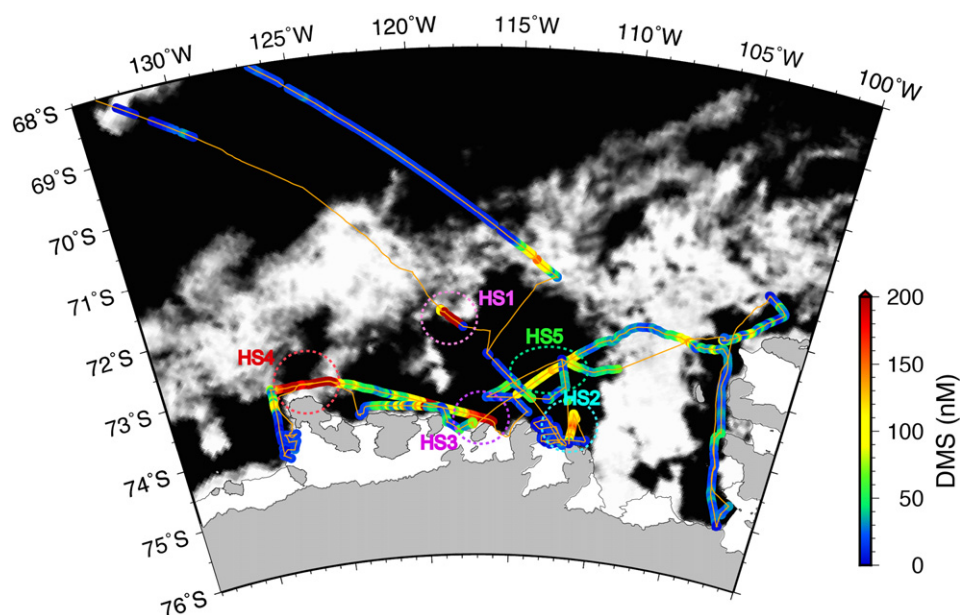


Fig. 4. Spatial distributions of DMS concentrations (contour map) throughout the Amundsen Sea surface waters from Jan 14 to Feb 10. The five hotspot (HS) sites are presented, where the mean DMS concentrations are > 150 nM.

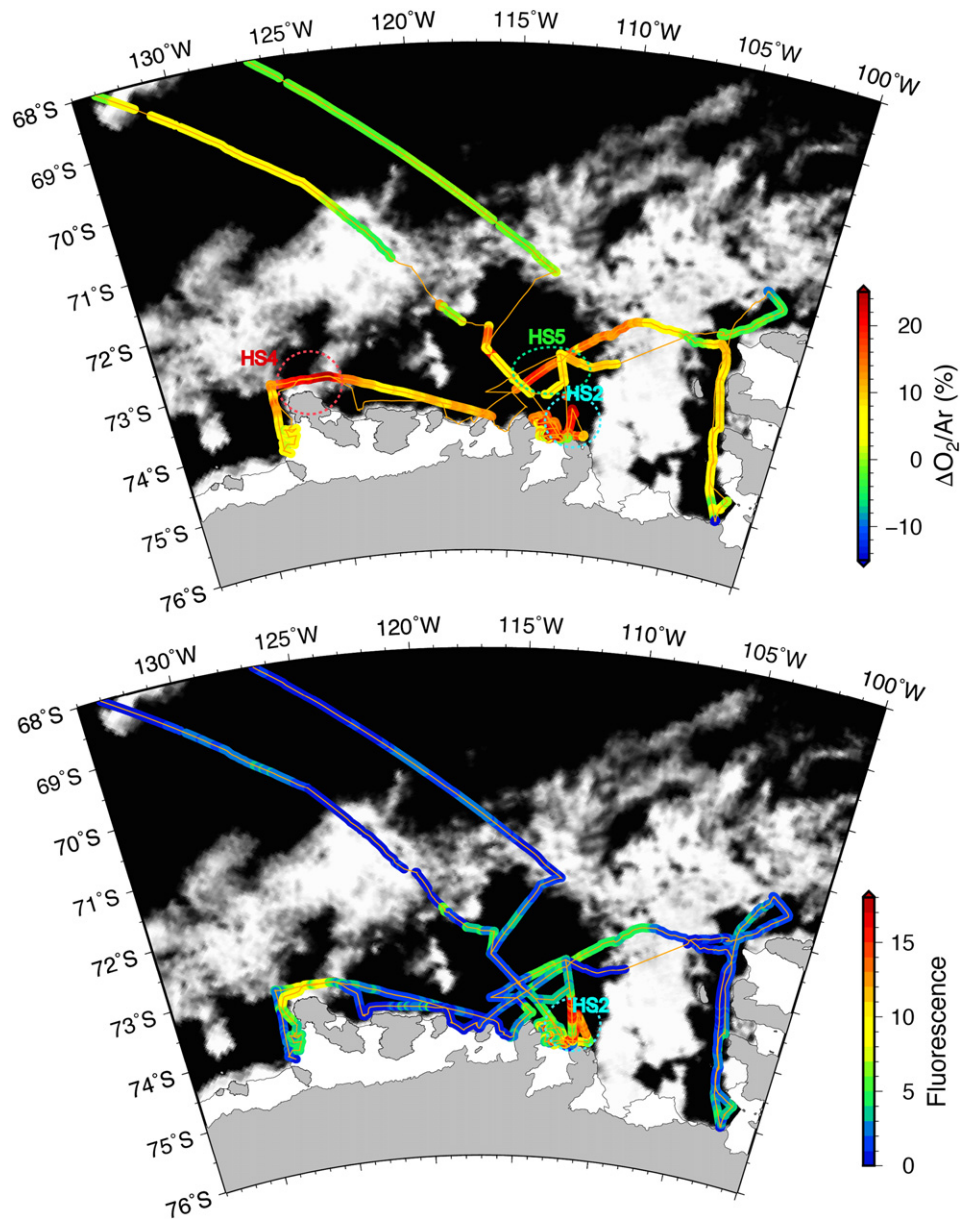


Fig. 5. Spatial distributions of $\Delta O_2/Ar$ (%) (upper figure) and fluorescence (below figure) (contours) values throughout the Amundsen Sea surface waters from Jan 14 to Feb 10.

in other ice shelf regions because of low productivity (almost $\sim 0\%$ of $\Delta O_2/Ar$ at surface in these regions) (Figs. 6 and S1).

During the revisit sampling period, Feb. 5th to 8th (stations 29, 27, 12, and 8, are denoted as stations 29re, 27re, 12re, and 8re, respectively), DMS concentrations in the surface water of the DT region were almost 50 nM, lower than the average DMS concentrations during first sampling in January (110 nM in the stations 8–26). DMS levels eventually reached below the limit of detection (~ 1 nM) at station 8 (Fig. S1). However, the $\Delta O_2/Ar$ and chlorophyll concentrations were lowest during this period, indicating the final stage of summer bloom. This indicates that the biological productivity and associated DMS productions show short-term scale (1 to 2 weeks) variability during late summer. Similarly, DMS concentrations in PIIS (stations 63 and 64 on Feb 3rd) were 30–50 nM (Fig. S1), which were similar to the average level throughout the Amundsen Sea, even though the productivity was also lowest in this region, almost $\sim 0\%$ of $\Delta O_2/Ar$. These results indicate that there are time lags between the *Phaeocystis* bloom and related DMS production.

4. Discussion

4.1. Factors leading to DMS hotspots in the Amundsen Sea surface

In HS1 site, considering that the other parts of the central polynya region were still ice covered ($>60\%$ ice content) and not completely open during this period (Fig. 3), the sudden and first local ice melting in this region could provoke concentrated production of plankton albeit the low mean chlorophyll of the ambient region.

In HS2 site, the dominance of *P. antarctica* ($>90\%$ of abundance) seems to result in high DMS (up to 150 nM) with highest biomass relative to the nearby DIS region (Figs. 3 and 5). Here, we note that our phytoplankton composition data are unpublished yet. However, these trends in phytoplankton assemblage with significant spatial variability in our study region has been consistently observed in recent years, 2012–2014 (Lee et al., 2016a,b).

In HS3 site, the complete sea ice-free condition (0% sea-ice concentration) of HS3 region seems to be attributable to the significant

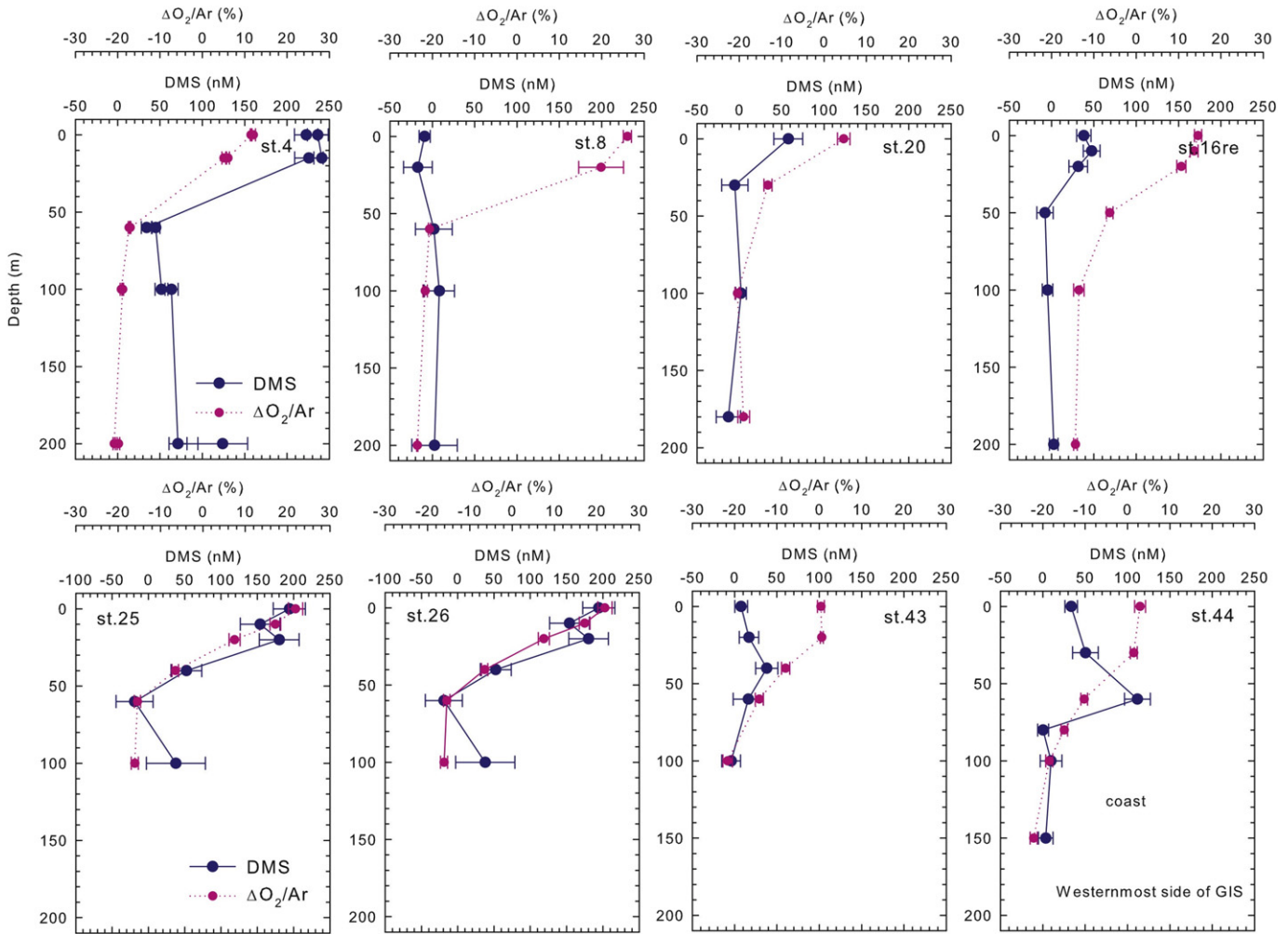


Fig. 6. Vertical profiles of DMS (blue dots and lines) and $\Delta O_2/Ar$ (%) (pink dots and dotted lines) for the some selected CTD cast stations. The uncertainty of each dataset is expressed by the 1-sigma (1σ) error bar. Vertical profiles of DMS (and $\Delta O_2/Ar$ (%)) and hydrography for all stations were in Figs. S1 and S2, respectively.

production of DMS (Figs. 3 and 4). However, chlorophyll and O_2 productions are not higher than other GIS regions (and also *P. antarctica* is not the dominant species at HS3). This result probably result from the exhaustion of nutrient directly after the peak blooming period, although the main factors elevating higher DMS in this region is not clear, yet.

On the contrary, the HS4 site seems to be coincidence with the peak bloom period based upon an optimum sea ice condition as spring bloom because both the chlorophyll and $\Delta O_2/Ar$ were clearly higher than other GIS region. Overall, our underway track seems to coincide with the peak bloom period near the GIS polynya region (especially, HS3 and HS4 sites), resulting in the highest $\Delta O_2/Ar$ ratio ($>20\%$) (Figs. 3–5).

Previous work suggests that the higher SST may affect the substantial DMS production (positive correlation between DMS and SST; Lana et al., 2011). Thus, the relatively higher SST ($0.5\text{--}0.7\text{ }^\circ\text{C}$) in HS5 site was likely to be responsible for the higher productivity (Fig. S3).

However, the significantly lower DMS concentrations in other DT region and polynya center seemed to be associated with the phytoplankton assemblage. For example, *P. antarctica* is not the predominant species (Lee et al., 2016a,b) in most of the DT, DIS, and polynya center region (stations 8 to 22 on Jan 17 to 23, Fig. 3).

The DMS flux in this study was 2–3 times higher than those in previous studies in the Ross Sea in 2006 ($0.040 \pm 0.020\text{ mmol m}^{-2}\text{ d}^{-1}$) and the Amundsen Sea in 2009 ($0.023 \pm 0.038\text{ mmol m}^{-2}\text{ d}^{-1}$)

(Tortell et al., 2011, 2012) and also compiled mean Southern Ocean data (Jarníková and Tortell, 2016). Because of the different observation locations, direct comparisons among these previous results are not easy. Although the domains of previous estimates reported by Tortell et al. (2012) were limited to the Amundsen Sea Polynya region ($0.058 \pm 0.130\text{ mmol m}^{-2}\text{ d}^{-1}$), our DMS flux ($0.085 \pm 0.119\text{ mmol m}^{-2}\text{ d}^{-1}$) is comparable within an order of magnitude.

Overall, the time series of underway observations (Fig. 3) showed that some biological factors (e.g., $\Delta O_2/Ar$ and fluorescence) are qualitatively having a close relationship with DMS. However, none of the environmental variables could clearly explain the DMS variation from correlation analyses (Fig. S4). There were weak or no correlations. Perhaps the time lag between the change of DMS and other environmental variables may explain the poor correlations; previous research reported that typical time lag between peak DMS and peak phytoplankton biomass are generally several days (Gabric et al., 1993). In addition, the DMS, $\Delta O_2/Ar$ ratio, and fluorescence showed opposite trends with sea ice content. This result is attributed to the fact that a sea ice melting can result in the production of substantial amounts of DMS, accompanied by O_2 and other trace gases from biological processes. The ubiquitous distributions of DMS hotspots (Figs. 3–5) are likely to be directly and mostly related to the spatial variability or physiological characteristics of phytoplankton assemblages in the study region.

4.2. Factors controlling vertical DMS distributions in the Amundsen Sea water column

In the DT region, there is significant discrepancy of DMS levels between station 4 (highest DMS near HS1) and station 8 (closed to 0 nM) despite of the local proximity between station 4 and station 8 (Fig. 6). The SIC were ~0% at station 4 but ~50% at station 8 (Fig. 3). Thus, this result implies that the beginning of ice melting (Section 3.1) in the shelf break region (near station 4) causes an abrupt bloom of *Phaeocystis* that has been delayed during the sea-ice forming winter season. In other DT region, DMS concentrations were consistently distributed with ~50 nM at the surface.

On the eastern side of DT (stations 23 to 26), near HS2 site, even though there were no distinct oxygen anomalies below a depth of 50 m, some elevated DMS concentrations were detected at a depth of 100 m (Figs. 6 and S1). These substantial enhancements of DMS concentrations might be associated with influences of physical water mixing at this depth, such as return flow of bottom water from ice shelves (Jenkins et al., 2010; Jacobs et al., 2011).

Interestingly, DMS values abruptly elevated at a depth of 50 m in the westernmost part of GIS (stations 42 to 44) (Figs. 6 and S1). Considering that all these stations showed similar vertical distributions (DMS anomaly at 50 m depth), the elevated DMS at mid depths might be related to a laterally transported DMS by water mixing. This trend in lateral transport of DMS in deep water was also observed in Ross Sea (Rellingner et al., 2009), even though there is no clear hydrographic evidence in this study, yet.

4.3. Comparisons of DMS distributions with previous study

Across our sampling region, we observed a noticeable variability of DMS and the $\Delta\text{O}_2/\text{Ar}$ ratio in surface waters and water columns of the Amundsen Sea. Especially, for the full data set, the DMS varied largely over more than two orders of magnitude, (>3–400 nM). The mean and median concentrations of DMS were 37 ± 76 nM and 20 nM, respectively. DMS levels in this work are similar to previous results by Tortell et al. (2012) (<1 nM to ~350 nM with mean and median values of 36 ± 54 nM and 16 nM, respectively). On the other hand, the $\Delta\text{O}_2/\text{Ar}$ in the Amundsen Sea surface waters ranged from ~20–30% with mean and median values of $4.3 \pm 5.9\%$ and 2.5%, respectively (Figs. 3–5). These values were about two times lower than the previous results by Tortell et al. (2012) ($8.6 \pm 16.6\%$) in the Amundsen Sea. Comparatively, nearly two-fold lower $\Delta\text{O}_2/\text{Ar}$ in this work seems to be due to some factors. For instance, i) during the cruise, the sea-ice zone was relatively larger than the mean of past years. ii) The inter-annual variability of wind strength is also a likely factor influencing this discrepancy of $\Delta\text{O}_2/\text{Ar}$ ratio (i.e., higher wind speed causes a lower $\Delta\text{O}_2/\text{Ar}$ due to rapid gas exchange under same biological conditions). Also, iii) this study additionally covers the western part of GIS compared to the previous work of Tortell et al. (2012) in which the productivity and related chlorophyll concentrations were lowest in the entire Amundsen Sea water columns.

Tortell et al. (2012) also presented the spatial distributions of DMS in the Amundsen Sea surface waters in 2009 for the first time. During that period, across the open polynya waters and sea ice zone (SIZ), $\Delta\text{O}_2/\text{Ar}$ ranged ~40 to 40% (mean 8.6%) and DMS concentrations varied from <1 to <350 nM. We note that our overall DMS data were distinctly higher than those of Tortell et al. (2012) (maximum ~150 nM) from the 2009 Amundsen cruise, although there was a difference between each cruise track. The higher DMS in this work might be due to inter-annual variations of hydrographic differences affected by El Niño Southern Oscillation, Southern Annular Mode, sea-ice conditions, and so on. For example, the significantly higher average SST during our cruise than that in 2009 (Fig. S5, ERA-interim re-analysis from Jan 15 to Feb 15, <http://www.ecmwf.int/en/research/climate-reanalysis/era-interim>) may result in substantially elevated DMS than 2009 based on the fact

that SST is highly correlated with surface DMS concentration (Toole and Siegel, 2004). In addition, especially in the polynya center along the DT (Jan 17–20), DMS concentrations were significantly lower than those of Tortell et al. (2012) in same area. This lower DMS period in the DT region coincided with the sea-ice melting stage. However, the DMS concentrations in this region increased during Feb 5–8 at the revisit stations (stations 12 and 8, Feb 7–8), though there were significant sea-ice formations (20–60% of SIC). This result suggests that there may be some time lags (several days) between initial blooms of *P. antarctica* at the first polynya formation and resultant productions of DMS (Gabric et al., 1993).

Tortell et al. (2012) reported that there was a clear distinction of DMS, $\Delta\text{O}_2/\text{Ar}$, and pCO_2 values between open polynya waters, pack ice, and the pelagic zone in the Southern Ocean. According to that result, the higher DMS and $\Delta\text{O}_2/\text{Ar}$ were usually distributed in the polynya zone, whereas the significantly higher pCO_2 were usually shown in the pack ice zone. For example, the mode (highest frequency) of DMS and $\Delta\text{O}_2/\text{Ar}$ were shown at 10–30 nM and 10–30%, respectively, in the polynya region and at 3–5 nM and ~10–0% in the pack ice region. On the other hand, in this study, both the polynya (<15% of SIC) and SIZ ($\geq 15\%$ of SIC) showed multi-modal distributions of DMS, within the range of 5–50 nM (Fig. 7). The mode of $\Delta\text{O}_2/\text{Ar}$ was 0–2% in both the polynya and SIZ. That is, in contrast to the results of Tortell et al. (2012), both DMS and $\Delta\text{O}_2/\text{Ar}$ have no clear distinction between regions, and the most common values of both polynya and sea-ice zone were shown to have similar ranges (Fig. 7).

In contrast to the results of Tortell et al. (2012), in this study the indistinct trends of DMS and $\Delta\text{O}_2/\text{Ar}$ frequencies from each domain seem to be related to temporal (inter-annual) variations of phytoplankton assemblages, referred to here as a relative less biomass *P. antarctica*. Considering that phytoplankton assemblages were dominated by the colonial haptophyte *P. antarctica* (with lesser biomass of diatoms found throughout the polynya and SIZ) at most sampling stations in 2009, the biomass of diatoms are comparable to *P. antarctica* in most of Amundsen Sea Polynya regions during this cruise, 2016 (unpublished data). This suggests, in comparison with the previous study, the production of DMSP subsequent to the growth of *P. antarctica* was not as rapid and explosive as before, because of intense competition with diatoms. Moreover, there could be some other factors causing the annual difference of DMS in each domain. For example, i) the totally sea-ice free regions were smaller than average years, instead, SIZ with 15–75% SIC continued during the whole cruise, Jan. to Feb. (Fig. 3) or ii) our sampling period could have been after the peak bloom season (can be in early Jan.); as such, differences in $\Delta\text{O}_2/\text{Ar}$ would have been invisible during the whole sampling period.

5. Concluding remarks

The horizontal (underway) and vertical (discrete bottle samples) distributions of DMS in the upper water column of the entire Amundsen Sea were investigated during the austral summer (Jan.–Feb.) of 2016 using MIMS on the Korean icebreaker R/V *Araon*. The concentrations of DMS in Amundsen surface water varied from 2 to 300 nM. Overall, the horizontal and vertical trends of DMS are well consistent with those of chlorophyll and $\Delta\text{O}_2/\text{Ar}$. Interestingly, DMS in surface water near DIS and GIS regions was higher than that in the polynya center along DT, which is in agreement with Tortell et al. (2012). In this study, we covered wider DMS survey regions in the Amundsen Sea than those of previous studies. As a result, the highest concentrations of DMS (up to 300 nM) were observed in the polynya mouth and near the GIS surface. Consequently, we discovered that there are still significant amount of DMS being produced in the Amundsen Sea, regardless of its distinct spatiotemporal variability. Nevertheless, observations of DMS are evidently lacking because of the limited accessibility of the polar ocean, and thus, significance of DMS flux in Southern Ocean is still largely underestimated. More extensive studies are necessary to

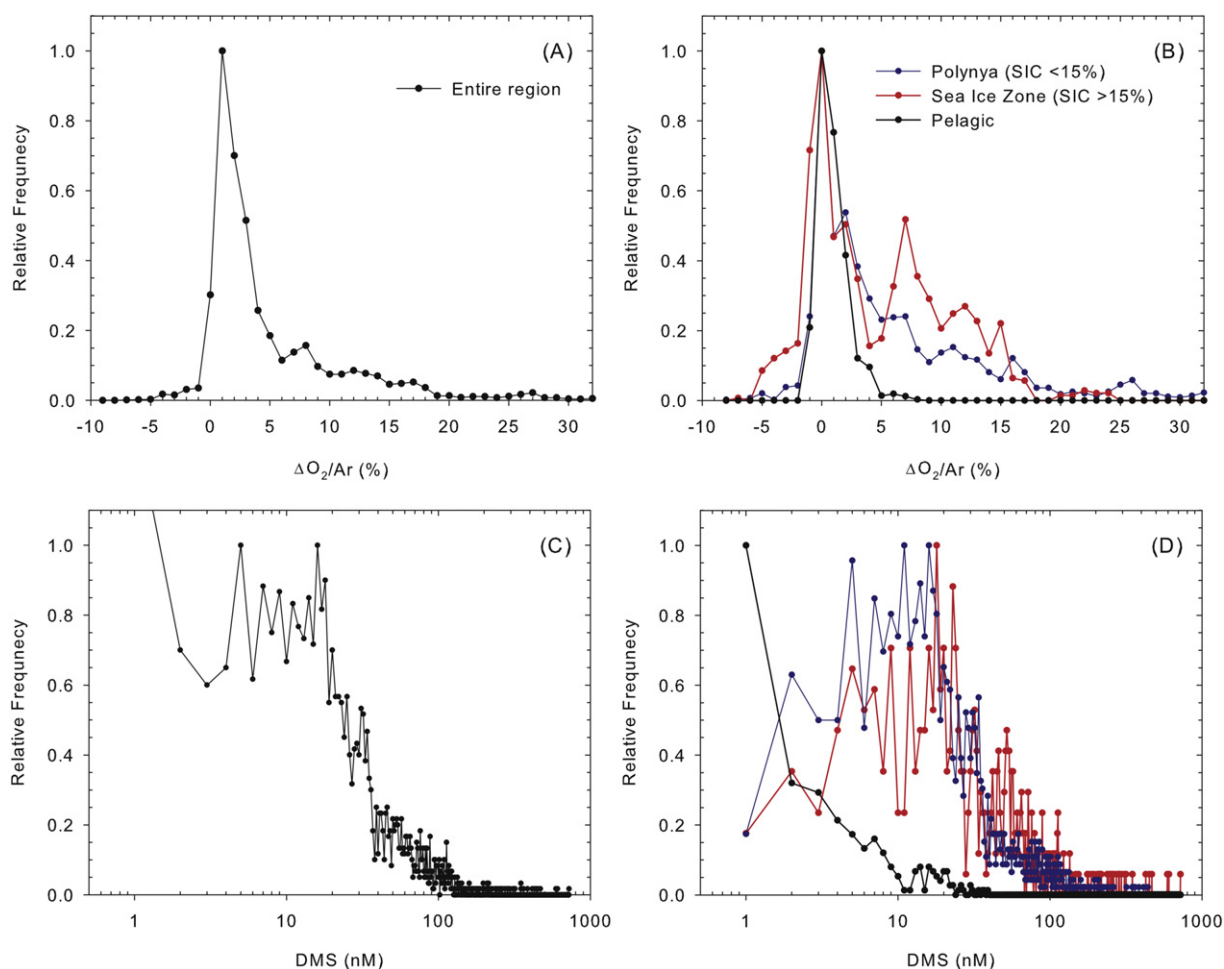


Fig. 7. Frequency distributions of $\Delta O_2/Ar$ (%) and DMS across our entire survey region (panels A and C, respectively) and for individual sampling domains (panels B and D, respectively). The domains, polynya and sea ice zone (SIZ), were distinguished by sea ice concentrations (SIC) of 15%. All frequencies are normalized to a maximum value of 1 to facilitate comparisons between the subplots. Note the logarithmic \times scaling on panels (C) and (D).

quantify the regional scales of DMS fluxes, to identify the variability of DMS biogeochemistry, and to evaluate their biogeochemical and climatological consequences under the continuous changing conditions in the polar oceans in the future.

Acknowledgements

We thank the captain and all the crewmembers of Icebreaker R/V *Araon*, who helped with sampling onboard. All datasets used in this paper are available upon request from the corresponding authors (hahm@pusan.ac.kr or keyhongpark@kopri.re.kr). This work was mainly supported by grants from the Korea Polar Research Institute (PE17060 and PE17120). L. Chen and M. Zhang were supported by National Natural Science Foundation of China (NSFC) 41476172 and D. Hahm was partially supported by Pusan National University Research Grant, 2016.

Appendix A. Supplementary data

Supplementary data to this article can be found online at <http://dx.doi.org/10.1016/j.scitotenv.2017.01.165>.

References

Alderkamp, A.C., Mills, M.M., van Dijken, G.L., Laan, P., Thuróczy, C.E., Gerringa, L.J., ... Arrigo, K.R., 2012. Iron from melting glaciers fuels phytoplankton blooms in the Amundsen Sea (Southern Ocean): phytoplankton characteristics and productivity. *Deep-Sea Res. II Top. Stud. Oceanogr.* 71, 32–48.

Arrigo, K.R., Van Dijken, G.L., 2003. Phytoplankton dynamics within 37 Antarctic coastal polynya systems. *J. Geophys. Res. Oceans* 108 (C8).

Arrigo, K.R., Worthen, D., Schnell, A., Lizotte, M.P., 1998. Primary production in Southern Ocean waters. *J. Geophys. Res. Oceans* 103 (C8), 15587–15600.

Bopp, L., Boucher, O., Aumont, O., Belviso, S., Dufresne, J.L., Pham, M., Monfray, P., 2004. Will marine dimethyl sulfide emissions amplify or alleviate global warming? A model study. *Can. J. Fish. Aquat. Sci.* 61 (5), 826–835.

Boyd, P.W., 2002. The role of iron in the biogeochemistry of the Southern Ocean and equatorial Pacific: a comparison of in situ iron enrichments. *Deep-Sea Res. II Top. Stud. Oceanogr.* 49 (9), 1803–1821.

Cameron-Smith, P., Elliott, S., Maltrud, M., Erickson, D., Wingenter, O., 2011. Changes in dimethyl sulfide oceanic distribution due to climate change. *Geophys. Res. Lett.* 38 (7).

Charlson, R.J., Lovelock, J.E., Andreae, M.O., Warren, S.G., 1987. Oceanic phytoplankton, atmospheric sulphur, cloud albedo and climate. *Nature* 326 (6114), 655–661.

Craig, H., Hayward, T., 1987. Oxygen supersaturation in the ocean: biological versus physical contributions. *Science* 235 (4785), 199–202.

DiTullio, G.R., 1996. Dimethylsulfide concentrations in the southern Ross Sea during austral summer 1995–1996. *Antarct. J. US* 31 (2), 127–128.

DiTullio, G.R., Smith, W.O., 1995. Relationship between dimethyl sulfide and phytoplankton pigment concentrations in the Ross Sea, Antarctica. *Deep-Sea Res. I Oceanogr. Res. Pap.* 42 (6), 873–892.

Ducklow, H.W., Wilson, S.E., Post, A.F., Stammerjohn, S.E., Erickson, M., Lee, S., Yager, P.L., 2015. Particle flux on the continental shelf in the Amundsen Sea Polynya and Western Antarctic Peninsula. *Elementa* 3 (1), 000046.

Gabric, A., Murray, N., Stone, L., Kohl, M., 1993. Modelling the production of dimethylsulfide during a phytoplankton bloom. *J. Geophys. Res. Oceans* 98 (C12), 22,805–22,816.

Gerringa, L.J., Alderkamp, A.C., Laan, P., Thuróczy, C.E., De Baar, H.J., Mills, M.M., ... Arrigo, K.R., 2012. Iron from melting glaciers fuels the phytoplankton blooms in Amundsen Sea (Southern Ocean): iron biogeochemistry. *Deep-Sea Res. II Top. Stud. Oceanogr.* 71, 16–31.

Jacobs, S.S., Jenkins, A., Giulivi, C.F., Dutrieux, P., 2011. Stronger ocean circulation and increased melting under Pine Island Glacier ice shelf. *Nat. Geosci.* 4 (8), 519–523.

Jarníková, T., Tortell, P.D., 2016. Towards a revised climatology of summertime dimethylsulfide concentrations and sea–air fluxes in the Southern Ocean. *Environ. Chem.* 13 (2), 364–378.

- Jenkins, A., Dutrieux, P., Jacobs, S.S., McPhail, S.D., Perrett, J.R., Webb, A.T., White, D., 2010. Observations beneath Pine Island Glacier in West Antarctica and implications for its retreat. *Nat. Geosci.* 3 (7), 468–472.
- Kettle, A.J., Andreae, M.O., Amouroux, D., Andreae, T.W., Bates, T.S., Berresheim, H., ... Helas, G., 1999. A global database of sea surface dimethylsulfide (DMS) measurements and a procedure to predict sea surface DMS as a function of latitude, longitude, and month. *Glob. Biogeochem. Cycles* 13 (2), 399–444.
- Kim, I., Hamm, D., Rhee, T.S., Kim, T.W., Kim, C.S., Lee, S.H., 2016. The distribution of glacial meltwater in the Amundsen Sea, Antarctica, revealed by dissolved helium and neon. *J. Geophys. Res.* 121, 1654–1666.
- Lana, A., Bell, T.G., Simó, R., Vallina, S.M., Ballabrera-Poy, J., Kettle, A.J., ... Johnson, J.E., 2011. An updated climatology of surface dimethylsulfide concentrations and emission fluxes in the global ocean. *Glob. Biogeochem. Cycles* 25 (1).
- Lee, Y., Yang, E.J., Park, J., Jung, J., Kim, T.W., Lee, S., 2016a. Physical-biological coupling in the Amundsen Sea, Antarctica: influence of physical factors on phytoplankton community structure and biomass. *Deep-Sea Res. I Oceanogr. Res. Pap.* 117, 51–60.
- Lee, Y.C., Park, M.O., Jung, J., Yang, E.J., Lee, S.H., 2016b. Taxonomic variability of phytoplankton and relationship with production of CDOM in the polynya of the Amundsen Sea, Antarctica. *Deep-Sea Res. II Top. Stud. Oceanogr.* 123, 30–41.
- Randall-Goodwin, E., Meredith, M.P., Jenkins, A., Yager, P.L., Sherrell, R.M., Abrahamsen, E.P., ... Alderkamp, A.C., 2015. Freshwater distributions and water mass structure in the Amundsen Sea Polynya region, Antarctica. *Elementa* 3 (1), 000065.
- Rellinger, A.N., Kiene, R.P., del Valle, D.A., Kieber, D.J., Slezak, D., Harada, H., ... Brinkley, J., 2009. Occurrence and turnover of DMSP and DMS in deep waters of the Ross Sea, Antarctica. *Deep-Sea Res. I Oceanogr. Res. Pap.* 56 (5), 686–702.
- Rignot, E., Jacobs, S., Mouginot, J., Scheuchl, B., 2013. Ice-shelf melting around Antarctica. *Science* 341 (6143), 266–270.
- Saltzman, E.S., King, D.B., Holmen, K., Leck, C., 1993. Experimental determination of the diffusion coefficient of dimethyl sulfide in water. *J. Geophys. Res. Oceans* 98 (C9), 16,481–16,486.
- Spreen, G., Kaleschke, L., Heygster, G., 2008. Sea ice remote sensing using AMSR-E 89 GHz channels. *J. Geophys. Res.* 113, C02S03.
- Stefels, J., 2009. Chapter 11: determination of DMS, DMSP, and DMSO in seawater. In: Wurl, O. (Ed.), *Practical Guidelines for the Analysis of Seawater*. CRC Press, FL, pp. 223–234.
- Toole, D.A., Siegel, D.A., 2004. Light-driven cycling of dimethylsulfide (DMS) in the Sargasso Sea: Closing the loop. *Geophys. Res. Lett.* 31, L09308. <http://dx.doi.org/10.1029/2004GL019581>.
- Tortell, P.D., 2005. Dissolved gas measurements in oceanic waters made by membrane inlet mass spectrometry. *Limnol. Oceanogr. Methods* 3 (1), 24–37.
- Tortell, P.D., Guéguen, C., Long, M.C., Payne, C.D., Lee, P., DiTullio, G.R., 2011. Spatial variability and temporal dynamics of surface water pCO₂, ΔO₂/Ar and dimethyl sulfide in the Ross Sea, Antarctica. *Deep-Sea Res. I Oceanogr. Res. Pap.* 58 (3), 241–259.
- Tortell, P.D., Long, M.C., Payne, C.D., Alderkamp, A.C., Dutrieux, P., Arrigo, K.R., 2012. Spatial distribution of pCO₂, ΔO₂/Ar and dimethyl sulfide (DMS) in polynya waters and the sea ice zone of the Amundsen Sea, Antarctica. *Deep-Sea Res. II Top. Stud. Oceanogr.* 71, 77–93.
- Van Boekel, J.S.W., Stefels, W.H.M., 1993. Production of DMS from dissolved DMSP in axenic cultures of the marine phytoplankton species *Phaeocystis* sp. *Mar. Ecol. Prog. Ser.* 97, 11–18.
- Wanninkhof, R., 1992. Relationship between wind speed and gas exchange over the ocean. *J. Geophys. Res. Oceans* 97 (C5), 7373–7382.